European Radiology (2019) 29:3638–3646
https://doi.org/10.1007/s00330-019-06079-x

CARDIAC

# Epicardial fat volume measured on nongated chest CT is a predictor of coronary artery disease

Yasunori Nagayama[1] · Naoki Nakamura[2] · Ryo Itatani[2] · Seitaro Oda[1] · Shinichiro Kusunoki[2] · Hideo Takahashi[2] · Takeshi Nakaura[1] · Daisuke Utsunomiya[3] · Yasuyuki Yamashita[1]

Received: 26 September 2018 / Revised: 24 December 2018 / Accepted: 7 February 2019 / Published online: 11 March 2019


## Abstract

**Objective** To investigate whether epicardial fat volume (EFV) quantified on ECG-nongated noncontrast CT (nongated-NCCT) could be used as a reliable and reproducible predictor for coronary artery disease (CAD).

**Methods** One hundred seventeen subjects (65 men, mean age 66.6 ± 11.9 years) underwent coronary CT angiography (CCTA) and nongated-NCCT during a single session because of symptoms suggestive of CAD. Two observers independently quantified EFV on both images. Correlation between CCTA-EFV and nongated-NCCT-EFV was assessed using Pearson's correlation coefficient and Bland–Altman plots. Inter-observer agreement was analyzed using concordance correlation coefficients (CCC). Coronary risk factors including EFV were compared between CAD-positive (> 50% stenosis) and CAD-negative groups. The association between EFV and CAD was analyzed using multivariate logistic regression. ROC analysis was performed, and AUC was compared with DeLong's method.

**Results** Seventy-four subjects were diagnosed with CAD. An excellent correlation was noted between CCTA-EFV and nongated-NCCT-EFV ($r = 0.948$, $p < 0.001$), despite the systematic difference between both measurements (mean bias, 1.26). Inter-observer agreement was nearly perfect (CCC, 0.988 and 0.985 for CCTA and nongated-NCCT, respectively, $p < 0.001$). Significant differences were noted between subjects with versus without CAD in age, hypertension, and EFV on both types of images ($p \leq 0.026$). Multivariate analysis revealed that increased EFV on CCTA (odds ratio 1.185, $p = 0.003$) and nongated-NCCT (odds ratio 1.20, $p = 0.015$) was independently associated with CAD. There was no significant difference between CCTA-EFV and nongated-NCCT-EFV in AUC for the prediction of CAD (0.659 vs 0.665, $p = 0.706$).

**Conclusions** Despite the absence of ECG gating, EFV measured on NCCT may serve as a reproducible predictor for CAD with accuracy equivalent to EFV measured on CCTA.

**Key Points**

- *Despite the absence of ECG gating, the EFV on NCCT provides nearly perfect inter-observer reproducibility and shows excellent correlation with measurements on gated CCTA.*
- *EFV on nongated-NCCT may serve as an independent biomarker for predicting coronary artery disease with accuracy equivalent to that of EFV on gated CCTA.*

**Keywords** Multidetector computed tomography · Pericardium · Body fat distribution · Coronary artery disease · Predictive value of tests

✉ Yasunori Nagayama
y.nagayama1980@gmail.com

[1] Department of Diagnostic Radiology, Graduate School of Medical Sciences, Kumamoto University, 1-1-1, Honjo, Chuo-ku, Kumamoto 860-8556, Japan

[2] Department of Radiology, Minamata City General Hospital and Medical Center, 1-2-1, Tenjin-cho, Minamata 867-0041, Japan

[3] Department of Diagnostic Radiology, Yokohama City University Hospital, 3-9 Fukuura, Kanazawa-ku, Yokohama 236-0004, Japan

**Abbreviations**

| | |
|---|---|
| CAD | Coronary artery disease |
| CCTA | Coronary CT angiography |
| EF | Epicardial fat |
| EFV | Epicardial fat volume |
| NCCT | Noncontrast CT |

## Introduction

Epicardial fat (EF) is a metabolically active adipose tissue located between the myocardium and the visceral pericardium. EF shares its embryologic origin with visceral fat and has been considered an important source of proinflammatory chemokines and cytokines in the development of atherosclerosis [1, 2]. EF has been postulated to have direct paracrine or vasocrine effects on the coronary arteries, because of the anatomic proximity between these tissues, with no fascial barrier throughout most of their course [1–5]. Studies have demonstrated that increased EF volume (EFV) is independently associated with coronary atherosclerosis and may be used as an imaging biomarker for predicting coronary artery disease (CAD) [6–9].

Increasing awareness of the significant associations between the development of coronary atherosclerosis and increased EF has led to the implementation of various measurement strategies for the estimation of EF. Computed tomography (CT) is widely considered the preferable imaging modality for quantification of EFV, because of its high spatial resolution and wide availability [10, 11]. Traditionally, CT volumetric analysis of EF has been performed on electrocardiography (ECG)-gated cardiac scanning with or without contrast medium, so as to minimize the motion artifact and clearly depict the pericardium [5–18]. This has restricted the potential prognostic utility of EFV and related investigations in subjects who require assessment of coronary atherosclerosis.

Compared with ECG-gated cardiac scanning such as coronary CT angiography (CCTA) and calcium score scanning, noncontrast CT (NCCT) without ECG gating is performed far more commonly to evaluate the lungs and other structures for numerous clinical indications [19]. Nongated-NCCT may have some advantages over CCTA, such as lower exposure to radiation and the lack of a need for contrast medium. The coronary artery calcium scoring on nongated-NCCT has been shown to be beneficial toward predicting mortality risk and future cardiovascular events despite the inherent motion artifact [20, 21]. Additionally, nongated-NCCT permits quantification of other cardio-metabolic markers, such as extent of valvular calcification, pulmonary artery diameter, and amount of liver fat, all of which are associated with subclinical or clinical cardiovascular disease [17, 18, 22–24]. In this context, it may also afford a valuable opportunity to improve primary prevention care, if nongated-NCCT can allow the measurement of EFV for stratifying cardiovascular risk, with accuracy and reproducibility similar to those of dedicated cardiac CT. However, no study published to date has compared nongated-NCCT and CCTA in terms of predictive value or reproducibility of EFV quantification [25, 26].

The purpose of this study was to evaluate the reproducibility and feasibility of EFV measurement on nongated-NCCT, and to ascertain its predictive value for the presence of CAD using CCTA images as reference standard.

## Materials and methods

This retrospective study was approved by the institutional review board, and requirement for written informed consent was waived. All patients agreed to undergo clinically indicated CT examinations and consented for their medical records to be used for research purposes.

### Patients

During the period from January 2011 to December 2012, 145 patients with symptoms suggestive of CAD (e.g., chest pain, epigastric pain, or short breath) underwent ECG-gated CCTA examinations for the evaluation of coronary arteries and nongated-NCCT scans for ruling out the presence of extracardiac abnormalities possibly causing similar symptoms and other clinically significant abnormalities (e.g., lung cancer). Both examinations were clinically indicated by the physicians and were performed consecutively on the same day after obtaining informed consent from the patients. Patients with myocardial infarction history ($n = 10$), implanted coronary artery stent ($n = 10$), coronary bypass surgery ($n = 4$), or previous pacemaker implantation ($n = 4$) were excluded. One hundred and seventeen patients were ultimately included in the present study.

Information related to cardiovascular risk factors such as history of hypertension (systolic blood pressure ≥ 140 mmHg, diastolic blood pressure ≥ 90 mmHg, or current use of antihypertensive agents), dyslipidemia (low-density lipoprotein cholesterol ≥ 140 mg/dL on direct measurement, total cholesterol ≥ 220 mg/dL, or use of lipid-lowering drugs), history of diabetes mellitus (glycohemoglobin $A_{1c}$ level ≥ 6.5%, or use of hypoglycemic agent or insulin), and smoking history (defined as current or previous smoking) was obtained from all patients at the time of examination using standard physician-based questionnaires.

### Image acquisition

Two consecutive CT scans were performed using a 64-row multidetector CT scanner (Definition AS, Siemens Healthineers) in one session, without any change in the patient's body position. Patients with a heart rate of 65 beats per minute were given oral beta-blocker (propranolol, 20 mg) 1 h prior to the examination. All patients received nitroglycerin (0.3 mg) orally just prior to CT scan. At first, nongated-NCCT scan was performed with 120 kVp, 160 quality reference mAs (modulated by automated exposure control), 128 × 0.6 mm collimation, 0.5-s rotation time, 1.2 pitch, and 3-mm slice thickness. These images were acquired from the lung apex to the lower pole of the liver (mean scanning range, 46.2 ± 4.4 cm) in a cranio–caudal direction. Then, ECG-gated contrast-enhanced CCTA was performed with 120 kVp, 190 mAs (automated exposure control was not utilized), 128 × 0.6 mm collimation, 0.3-s rotation time, 0.18 pitch, and 0.75-mm slice

thickness. A bolus dose of the contrast medium iopamidol (Iopamiron-370; Bayer) was intravenously injected at 1 mL/kg body weight over 15 s, followed by 30 ml of normal saline flash. The CCTA image data were reconstructed with 75% of RR wave or particular optimal cardiac phase showing the minimum motion artifact. CCTA and nongated-NCCT data were reconstructed using a dedicated soft-tissue convolution kernel (B35f). Each reconstructed image was transferred to a workstation for postprocessing.

## Quantification of EFV

Methods for EFV quantification on both types of scans were performed with commercially available volumetric software (Virtual Place Plus; AZE), as previously described [5–8]. We defined EF as all adipose tissue located within the pericardium. EF area ($cm^2$) was measured every 10–15 mm from the mid-left atrium to the cardiac apex by manually tracing the pericardium, with attenuation ranging from − 190 to − 30 Hounsfield units (HU) defined as fat voxels. The software automatically interpolated between user-defined traces, and contours were manually adjusted to the pericardium if needed. EFV ($cm^3$) was automatically calculated as the summation of EF areas. All measurements were performed on CCTA and nongated-NCCT images (Fig. 1) by a radiologist with 10 years of experience in cardiac imaging. EFV was also quantified by a different radiologist with 10 years of experience in cardiac imaging, to evaluate inter-observer reproducibility for each image set. Operators were blinded to participant clinical data including the presence or absence of CAD. To reduce recall bias, the EFV quantification in CCTA and nongated-NCCT was performed on different days in random order by each operator.

## Assessment of CCTA

Based on the Society of Cardiovascular Computed Tomography (SCCT) 18 segments model [27], three major coronary arteries were analyzed on CCTA. Two board-certified radiologists with 7 and 14 years of experience, respectively, in cardiac imaging performed the analysis. The presence of coronary plaques and stenosis severity were visually evaluated using curved multi-planar reconstructions and cross-sectional images. We defined CAD as obstructive coronary stenosis, which was determined by the presence of at least one coronary artery stenosis > 50%, irrespective of plaque morphology [9, 14, 28, 29]. Coronary atherosclerotic plaques were classified as calcified plaque (plaque comprising only calcium or partially calcified) or non-calcified plaque (calcium free plaque). Patients with both non-calcified and calcified plaques were classified as patients with calcified plaques. In the case of a discrepancy between readers, consensus was reached by discussion.

## Statistical analysis

Statistical analyses were performed with MedCalc statistical software (MedCalc Software). Continuous variables are expressed as mean ± standard deviation, and proportions (%) were used for categorical variables. A paired Student's *t* test was used to compare differences in EFV obtained with the two acquisitions. Correlations between EFV as measured on the two types of scan were evaluated using Pearson's correlation coefficient. Bland–Altman analysis was also performed to determine the bias and limits of agreement between CCTA and the nongated-NCCT, with the natural log transformation of

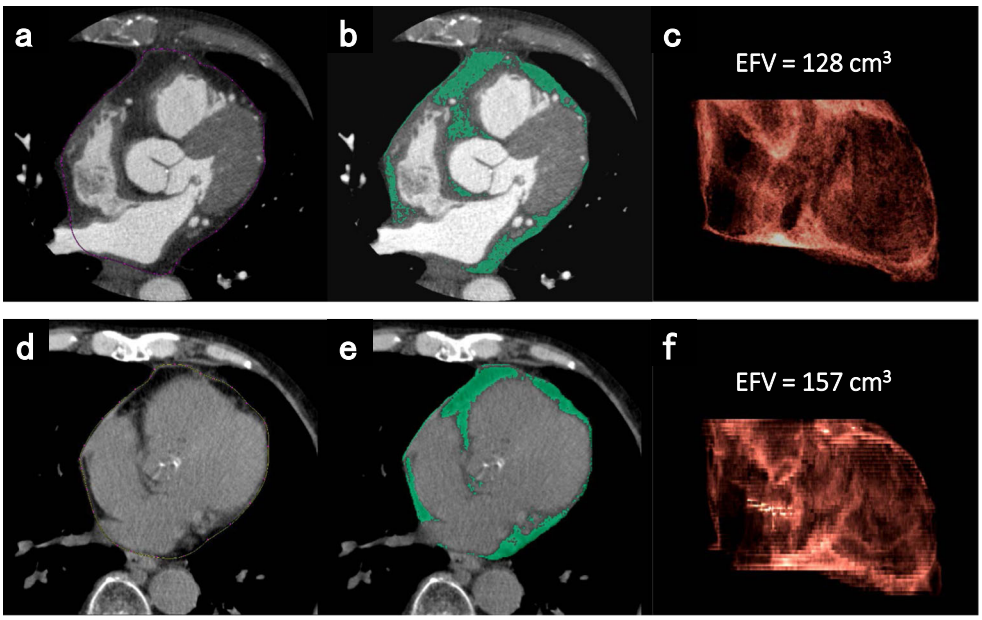


**Fig. 1** Quantification of epicardial fat volume (EFV) on coronary CT angiography (**a**–**c**) and nongated noncontrast CT (**d**–**f**) using semi-automated software. To determine a region of interest, the pericardium was manually traced on each slice from the mid-left atrium to the cardiac apex (**a**, **d**). Within the region of interest, fat voxels were identified using a threshold attenuation range of − 190 to − 30 HU (**b**, **e**). The EFV is automatically calculated by the software (**c**, **f**)

EFV being used to approximate a normal distribution [30–32]. Inter-observer reproducibility for the measurement of EFV was assessed with concordance correlation coefficients (CCC) and their 95% confidence intervals (CIs). Differences in the EFV among subjects with no plaque, calcified plaque, and non-calcified plaque were analyzed by using one-way ANOVA, using the Fisher LSD method for post hoc determination of significance. To analyze differences in demographics, traditional cardiovascular disease risk factors, and EFV between CAD-positive and CAD-negative groups, Student's *t* test or Mann–Whitney *U* test was used for continuous variables; the chi-square test was used for categorical variables. Univariate and multivariate logistic regression analyses were performed to examine the association of EFV on each type of scan with CAD. All variables considered to be clinically relevant risk factors (including age, sex, body mass index, diabetes, hypertension, dyslipidemia, and smoking history) were entered into the multivariable models irrespective of the *p* value in the univariate analysis in order to exclude any confounding effects. Odds ratios (ORs) and 95% CIs for CAD were calculated. Receiver operating characteristic (ROC) analysis was performed to determine cutoff values and calculate areas under the ROC curves (AUCs) for the prediction of CAD. AUC values were compared between CCTA and nongated-NCCT with DeLong's method [33]. $P < 0.05$ was considered statistically significant.

## Results

### Patient characteristics

Patient characteristics are summarized in Table 1. The mean age among included subjects was 66.6 ± 11.9 years. There were 65 male subjects (55.6%). There were 26 subjects with no plaque (22.2%), 71 with calcified plaque (60.7%), and 20 with non-calcified plaque (17.1%). A total of 74 patients (63.2%) were diagnosed with CAD on CCTA examinations. Among patients with CAD, one-vessel disease was demonstrated in 33 patients (44.6%), two-vessel disease in 32 (43.2%), and three-vessel disease in 9 (12.1%).

**Table 1** Clinical characteristics of included subjects ($n = 117$)

| Characteristic | N (%) or mean ± SD |
|---|---|
| Age (years) | 66.6 ± 11.9 |
| Male gender | 65 (55.6) |
| BMI (kg/m$^2$) | 24.2 ± 4.4 |
| Cardiovascular risk factors | |
| Diabetes mellitus | 53 (45.3) |
| Hypertension | 66 (56.4) |
| Dyslipidemia | 65 (55.6) |
| Smoking history | 44 (40.2) |
| CAD positive | 74 (63.2) |
| CCTA-EFV (cm$^3$) | 83.9 ± 36.3 |
| NCCT-EFV (cm$^3$) | 110.5 ± 46.6 |

*BMI* body mass index, *CAD* coronary artery disease, *CCTA* coronary CT angiography, *EFV* epicardial fat volume, *NCCT* nongated noncontrast CT

### Correlation between EFV as measured on CCTA and nongated-NCCT

Excellent correlation was found between EFV as measured on CCTA and nongated-NCCT images ($r = 0.965$, $p < 0.001$, Fig. 2), though mean EFV on CCTA was significantly lower than mean EFV on nongated-NCCT (83.9 ± 46.6 vs. 110.5 ± 36.9 cm$^3$, $p < 0.001$). Bland–Altman analysis showed a mean bias of 1.260, with limits of agreement ranging from 0.987 to 1.607, suggesting that EFV on nongated-NCCT scans was, on average, approximately 26% higher than EFV on CCTA scans [31, 32]. The corresponding plot of the log-transformed EFV difference against average is shown in Fig. 3.

### Inter-observer agreement for EFV quantification

CCC for inter-observer agreement for quantification of EFV was 0.988 (95% CI, 0.983–0.992) and 0.985 (95% CI, 0.979–0.989) for CCTA and nongated-NCCT, respectively. These values indicate that reproducibility of EFV measurement on both image sets was near perfect (Fig. 4).

### Comparison of EFV based on the plaque characteristics

The EFV in subjects with non-calcified (CCTA-EFV 106.2 ± 44.4 cm$^3$, NCCT-EFV 131.4 ± 52.7 cm$^3$) and calcified

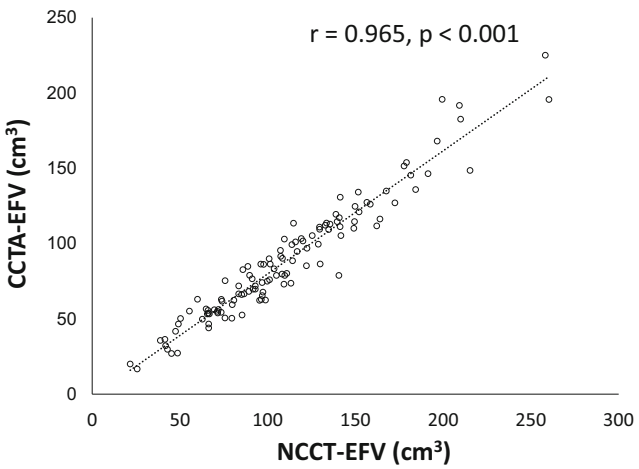


**Fig. 2** Correlation between epicardial fat volume (EFV) quantified on nongated noncontrast CT (NCCT-EFV) and coronary CT angiography (CCTA-EFV)

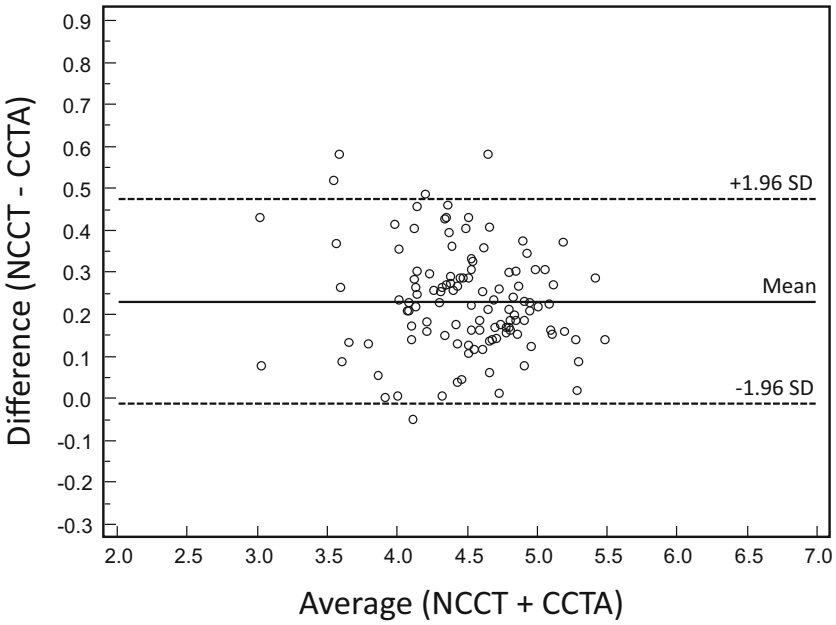


**Fig. 3** Bland–Altman plot of agreement between nongated noncontrast CT (NCCT) and coronary CT angiography (CCTA) using log-transformed epicardial fat volume. Log-transformed mean bias (center line), and lower and upper limits of agreement (top and bottom dashed lines) were 0.231, − 0.013, and 0.474, respectively. These values back-transform to mean bias 1.260, with limits of agreement ranging from 0.987 to 1.607

plaques (CCTA-EFV 90.3 ± 35.6 $cm^3$, NCCT-EFV 112.5 ± 42.0 $cm^3$) was significantly larger than that in those with no plaques (CCTA-EFV 69.6 ± 39.1 $cm^3$, NCCT-EFV 88.6 ± 46.4 $cm^3$) ($p \leq 0.022$). Subjects with non-calcified plaques had larger EFV than those with calcified plaques, although this difference did not attain statistically significant levels (CCTA-EFV: $p = 0.101$; NCCT-EFV: $p = 0.100$).

## Comparison of risk factors based on presence of CAD

Differences in risk factors, including the EFV, between the CAD-negative and CAD-positive groups are summarized in Table 2. Compared with subjects without CAD, subjects with CAD were significantly older ($p < 0.001$) and more likely to have hypertension ($p = 0.026$). The EFV measured on both CCTA and nongated-NCCT was significantly larger in subjects with CAD than in those without CAD ($p \leq 0.004$).

## Logistic regression analysis

The results of logistic regression analysis are summarized in Table 3. Univariate analysis showed a significant association between the presence of CAD and EFV measured on both CCTA (OR 1.175 [95% CI 1.045–1.321] per 10 $cm^3$, $p = 0.007$) and nongated-NCCT (OR 1.162 [95% CI 1.052–1.284] per 10 $cm^3$, $p = 0.003$). Even after adjustment for age, gender, BMI, diabetes mellitus, hypertension, dyslipidemia, and smoking history, increased EFV measured on both

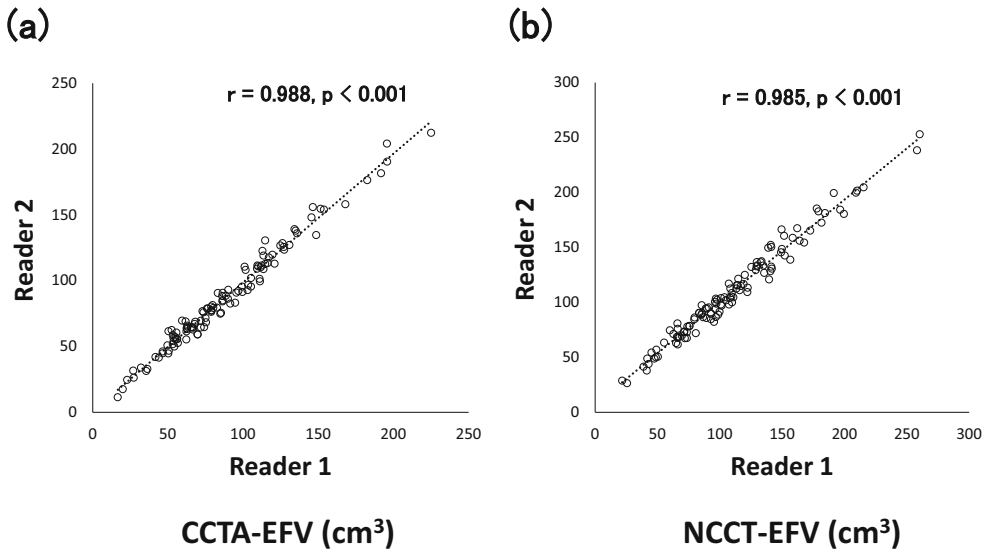


**Fig. 4** Inter-observer reproducibility for EFV quantification on coronary CT angiography (CCTA, **a**) and nongated noncontrast CT (NCCT, **b**)

**Table 2** Patient characteristics according to the presence or absence of coronary artery disease

| Characteristics | CAD positive ($n = 74$) | CAD negative ($n = 43$) | $p$ value |
|---|---|---|---|
| Age (years) | 69.1 ± 8.9 | 62 ± 11.8 | < 0.001[a] |
| Male gender | 45 (60.8) | 20 (46.5) | 0.191[b] |
| BMI (kg/m$^2$) | 24.3 ± 4.4 | 24.1 ± 3.5 | 0.814[a] |
| Cardiovascular risk factors | | | |
| Diabetes mellitus | 38 (52) | 15 (34) | 0.125[b] |
| Hypertension | 48 (64.9) | 18 (41.9) | 0.026[b] |
| Dyslipidemia | 45 (60.8) | 20 (46.5) | 0.191[b] |
| Smoking history | 30 (40) | 14 (32) | 0.508[b] |
| CCTA-EFV (cm$^3$) | 96.2 ± 40.2 | 75.1 ± 34.7 | 0.004[c] |
| NCCT-EFV (cm$^3$) | 120.5 ± 47.5 | 93.2 ± 39.9 | 0.003[c] |

Data are shown mean ± SD or number (%)

*BMI* body mass index, *CAD* coronary artery disease, *CCTA* coronary CT angiography, *EFV* epicardial fat volume, *NCCT* nongated noncontrast CT

[a] Student's $t$ test, [b] chi-square test, [c] Mann–Whitney $U$ test

CCTA (multivariate model 1, OR 1.185 [95% CI 1.009–1.392] per 10 cm$^3$, $p = 0.005$) and nongated-NCCT (multivariate model 2, OR 1.200 [95% CI 1.036–1.391] per 10 cm$^3$, $p = 0.015$) was still significantly associated with the presence of CAD.

### ROC analysis

ROC curves for EFV as a predictor of CAD are shown in Fig. 5. AUC values of EFV quantified on CCTA and nongated-NCCT for the prediction of CAD were 0.659 (cutoff value, 78.8 cm$^3$) and 0.665 (cutoff value, 101.0 cm$^3$), respectively. There was no significant difference in AUC values between both scanning types ($p = 0.706$).

## Discussion

Previous studies have shown that increased EFV is independently associated with coronary stenosis, myocardial ischemia, and major adverse cardiovascular events, irrespective of its association with traditional cardiovascular risk factors [6–9, 16]. Concordant with these findings, increased EFV was independently and proportionally associated with the presence of CAD in our study, even after adjustment for established cardiovascular risk factors. The most notable finding among the results presented above was that nongated-NCCT could be utilized to quantify EFV with almost perfect reproducibility, and EFV on nongated-NCCT could serve as an independent biomarker for the prediction of CAD, with accuracy equivalent to that of EFV on CCTA.

**Table 3** Results of univariate and multivariate logistic regression analysis

| Risk factors | Univariate analysis | | Multivariate analysis (model 1) | | Multivariate analysis (model 2) | |
|---|---|---|---|---|---|---|
| | OR (95% CI) | $p$ value | OR (95% CI) | $p$ value | OR (95% CI) | $p$ value |
| Age (per 1 year) | 1.073 (1.029–1.120) | 0.001 | 1.095 (1.039–1.154) | < 0.001 | 1.095 (1.039–1.154) | < 0.001 |
| Male gender | 1.785 (0.835–3.814) | 0.135 | 2.861 (0.888–9.219) | 0.078 | 2.889 (0.881–9.479) | 0.080 |
| BMI (per 1 kg/cm$^2$) | 1.011 (0.922–1.110) | 0.812 | 0.948 (0.833–1.079) | 0.420 | 0.918 (0.797–1.056) | 0.231 |
| Diabetes mellitus | 1.970 (0.908–4.278) | 0.086 | 1.964 (0.774–4.982) | 0.155 | 1.868 (0.732–4.767) | 0.191 |
| Hypertension | 2.564 (1.186–5.545) | 0.017 | 2.042 (0.810–5.151) | 0.130 | 1.952 (0.766–4.973) | 0.161 |
| Dyslipidemia | 1.785 (0.835–3.814) | 0.135 | 2.707 (1.019–7.191) | 0.046 | 2.866 (1.059–7.750) | 0.038 |
| Smoking history | 1.412 (0.642–3.108) | 0.391 | 0.701 (0.202–2.426) | 0.575 | 0.714 (0.203–2.513) | 0.600 |
| CCTA-EFV (per 10 cm$^3$) | 1.175 (1.045–1.321) | 0.007 | 1.185 (1.009–1.392) | 0.005 | – | – |
| NCCT-EFV (per 10 cm$^3$) | 1.162 (1.052–1.284) | 0.003 | – | – | 1.200 (1.036–1.391) | 0.015 |

Data are shown mean ± SD or number (%)

*BMI* body mass index, *CCTA* coronary CT angiography, *EFV* epicardial fat volume, *NCCT* nongated noncontrast CT

Model 1: traditional risk factors and EFV quantified on CCTA; model 2: traditional risk factors and EFV quantified on NCCT

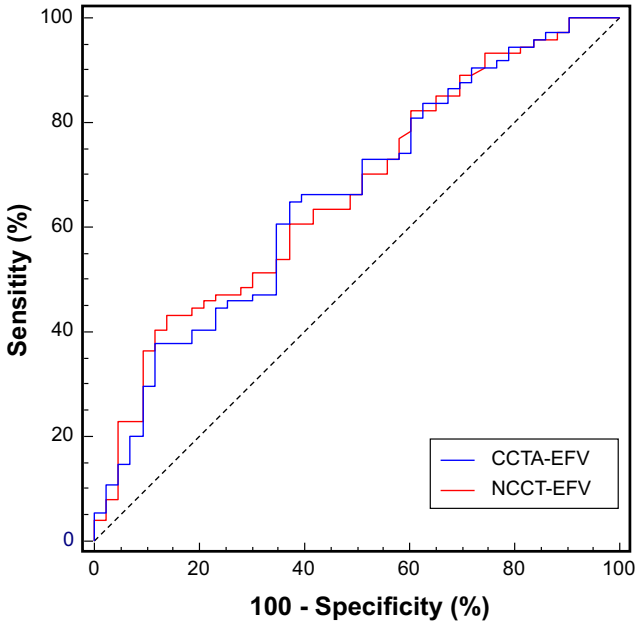


**Fig. 5** The receiver operating characteristic curves for epicardial fat volume (EFV), as quantified on coronary CT angiography (CCTA, blue line, cutoff value = 78.7 $cm^3$, area under the curve = 0.659) and nongated noncontrast CT (NCCT, red line, cutoff value = 101 $cm^3$, area under the curve = 0.665) to predict coronary artery disease

Traditionally, quantification of EF on CT examination is performed with ECG-gated scanning with or without contrast medium, which restricts the benefits of EF quantification to subjects who receive scanning protocols designed for evaluation of the coronary artery. To our knowledge, only two studies have suggested that the nongated-NCCT is potentially usable for the estimation of amount of EF as a substitution of ECG-gated cardiac CT [25, 26]. Lee et al demonstrated that EF area ($cm^2$) at the left main and right coronary artery ostium levels measured on nongated-NCCT can be potentially used for the prediction of coronary atherosclerosis in an asymptomatic population considered for self-referred lung cancer screening [26]. Despite their suggestive findings, the reported correlation between the EF area on nongated-NCCT and EFV on CCTA were relatively low ($r = 0.712–0.725$), probably because of asymmetrical and uniform distribution of EF [12, 15]. Additionally, the inter-observer reproducibility and the accuracy for the prediction of coronary atherosclerosis were not compared between the two scanning techniques. Yarza et al demonstrated that nongated-NCCT permits quantification of EFV with almost perfect concordance and reproducibility as ECG-gated noncontrast calcium-scoring scans [25]. Their findings were concordant with our findings although we used CCTA instead of calcium-scoring scans as reference ECG-gated images. Yarza et al did not investigate the association between EFV on nongated-NCCT and the presence of CAD, and thus its prognostic values remain to be assessed. Therefore, our study is the first to demonstrate that EFV on nongated-NCCT shows excellent correlation with EFV on CCTA ($r = 0.965$, $p < 0.001$), with almost perfect inter-operator reproducibility ($r = 0.987$, $p < 0.001$), and may serve as a prognostic marker for CAD with accuracy equivalent to EFV on CCTA (AUC 0.665 vs. 0.659, $p = 0.706$) in subjects clinically referred for CCTA scans.

We found that EFV as measured on nongated-NCCT was approximately 30% higher than that measured on CCTA, despite use of the same quantitative methodology. The Bland–Altman analysis also revealed an inherent systematic difference in EFV measurements between the two types of scans. Similar findings have been reported by Marwan et al and Grutta et al, who suggested that EFV was systematically underestimated on CCTA images owing to iodine enhancement, when compared with calcium-scoring scanning [5, 34]. Therefore, the attenuation thresholds for fat detection with semiautomatic software should be modified to mitigate the under- or overestimation, when absolute EFV values obtained from different types of scans are used as prognostic markers [5, 34]. In particular, Bucher et al suggested that the underestimation of EFV on CCTA images relative to gated-NCCT could be reconciled by the upper threshold modifications rather than by the lower threshold modifications [35]. Despite these implications, we decided to apply the upper threshold of − 30 HU for the CCTA as well as for the nongated-NCCT, because previous studies have typically used this threshold for CCTA, and demonstrated the significant association between CCTA-EFV and coronary atherosclerosis [7, 9, 12, 13, 36, 37]. In this context, our study showed that EFV measurements as determined with CCTA or nongated-NCCT have equivalent predictive value for risk estimation, when optimal cutoff values (CCTA, 78.8 $cm^3$; NCCT, 101.0 $cm^3$) for each image set are applied. Our findings are in line with the results of recent meta-analysis, which demonstrated that the predictive value for the presence of CAD did not differ according to scan type (ECG-gated NCCT or CCTA) used to quantify EFV [9].

In the present study, we could not compare the EFV values and its predictive performance between nongated- and gated-NCCT. During the observational period, gated-NCCT for calcium scoring was not routinely performed in our study population, because CCTA generally allows more comprehensive assessment of coronary atherosclerosis (e.g., the presence of calcified and non-calcified plaque as well as the severity of luminal stenosis). For the same reason, we could not correlate the EFV with calcium scores, which may serve as the preferable reference standard for the asymptomatic population potentially indicated for screening nongated-NCCT. Nevertheless, the calcium score alone may be insufficient in revealing the potential association between increased EFV and coronary atherosclerosis, because prior investigations have reported that increased EFV is associated with non-calcified plaque or obstructive CAD in population with zero calcium score [36, 37], but not with coronary calcification [9, 13]. Therefore, the presence of CAD, including non-calcified

plaque, may serve as an optimal and clinically relevant reference standard in this study.

The results of our study may have important clinical implications for preventive cardiology care. As nongated-NCCT is performed far more frequently than ECG-gated cardiac CT (i.e., CCTA or calcium-scoring scans) for various clinical indications [19], numerous individuals will have or already have their CT images that allow for the quantification of EFV, in addition to other cardio-metabolic health markers, such as the amount of liver fat [18, 24]. Thus, we can utilize all these image data to stratify the CAD risk without dedicated cardiac scanning, which usually requires additional cost, higher radiation exposure, and contrast medium administration. For example, our findings can be useful for hybrid PET/CT and SPECT/CT, where the nongated-NCCT scans are performed for accurate attenuation correction. EFV measured on these images is expected to improve cardiovascular risk stratification. In particular, quantifying EFV in combination with coronary calcium scoring on the same nongated-NCCT images may provide a more accurate method of risk stratification than would otherwise be possible, because EF may be associated with coronary atherosclerosis via pathologic signal pathways that differ from those involved in coronary artery calcification, such as the development of non-calcified and potentially unstable coronary plaques [9, 13, 36, 37]. Moreover, our results may promote large follow-up studies including subjects with various degree of CAD risks not previously indicated for cardiac scans, which may further elucidate pathophysiology and prognostic role of EF for the development of cardiovascular disease [5].

Beyond the retrospective design, several limitations of this study should be acknowledged. First, this was an observational study that included a relatively small sample size and was performed at a single center. Additional large-scale studies are required to validate and expand our results. Second, we could not evaluate the association between EFV and myocardial ischemia or cardiovascular mortality; rather, the presence of coronary stenosis on CCTA was used as an alternative endpoint. In order to determine whether EFV as measured on nongated-NCCT may be used to predict future major adverse cardiac events, additional large prospective outcome trials should be performed. Third, our results revealed that the predictive power of EFV alone for the detection of CAD was still limited, although EFV may be used as one of the clues for risk stratification of coronary atherosclerosis when CCTA images are unavailable. In clinical practice, however, EFV can be incrementally added to other clinical information such as traditional cardiovascular risk factors, which could improve predictive value for the presence of CAD [7, 36]. Finally, we evaluated the symptomatic population with a relatively high prevalence of CAD; thus, the association between EFV and CAD determined in our multivariate analysis may not be directly extrapolated to an asymptomatic population with different pretest probabilities. Nevertheless, the feasibility of nongated-NCCT shown in our study may accelerate the research including subjects with various degree of CAD risk. Such an investigation may reveal which kind of population would benefit most from EFV quantification for the prediction of CAD, future cardiac events, and mortality.

In conclusion, despite the absence of ECG gating, EFV measurements on NCCT are highly reproducible and almost perfectly correlated with those of gated CCTA images. EFV measurements on nongated-NCCT may therefore be used as a non-invasive imaging biomarker for the prediction of CAD. The results presented above suggest that EFV measurements on nongated-NCCT are as accurate as EFV measurements on CCTA for prediction of CAD. Thus, individuals who will have or already have nongated-NCCT images for other clinical indications may benefit from using EFV quantification to anticipate additional CAD risk without added cost and radiation exposure required for dedicated cardiac scans. Future studies should include a large sample size of patients not previously examined with dedicated cardiac scans, which may further elucidate the pathophysiology and prognostic role of EF for the development of cardiovascular disease.

**Funding** The authors state that this work has not received any funding.

## Compliance with ethical standards

**Guarantor** The scientific guarantor of this publication is Yasuyuki Yamashita.

**Conflict of interest** The authors of this manuscript declare no relationships with any companies, whose products or services may be related to the subject matter of the article.

**Statistics and biometry** No complex statistical methods were necessary for this paper.

**Informed consent** Written informed consent was waived by the Institutional Review Board.

**Ethical approval** Institutional Review Board approval was obtained.

**Methodology**
- retrospective
- observational
- performed at one institution



## References

1. Iacobellis G, Corradi D, Sharma AM (2005) Epicardial adipose tissue: anatomic, biomolecular and clinical relationships with the heart. Nat Clin Pract Cardiovasc Med 2:536–543

2. Sacks HS, Fain JN (2007) Human epicardial adipose tissue: a review. Am Heart J 153:907–917
3. Tavora F, Kutys R, Li L, Ripple M, Fowler D, Burke A (2010) Adventitial lymphocytic inflammation in human coronary arteries with intimal atherosclerosis. Cardiovasc Pathol 19:e61–e68
4. Konishi M, Sugiyama S, Sato Y et al (2010) Pericardial fat inflammation correlates with coronary artery disease. Atherosclerosis 213: 649–655
5. Marwan M, Achenbach S (2013) Quantification of epicardial fat by computed tomography: why, when and how? J Cardiovasc Comput Tomogr 7:3–10
6. Cheng VY, Dey D, Tamarappoo B et al (2010) Pericardial fat burden on ECG-gated noncontrast CT in asymptomatic patients who subsequently experience adverse cardiovascular events. JACC Cardiovasc Imaging 3:352–360
7. Konishi M, Sugiyama S, Sugamura K et al (2010) Association of pericardial fat accumulation rather than abdominal obesity with coronary atherosclerotic plaque formation in patients with suspected coronary artery disease. Atherosclerosis 209:573–578
8. Iwasaki K, Matsumoto T, Aono H, Furukawa H, Samukawa M (2011) Relationship between epicardial fat measured by 64-multidetector computed tomography and coronary artery disease. Clin Cardiol 34:166–171
9. Mancio J, Azevedo D, Saraiva F et al (2018) Epicardial adipose tissue volume assessed by computed tomography and coronary artery disease: a systematic review and meta-analysis. Eur Heart J Cardiovasc Imaging 19:490–497
10. Saura D, Oliva MJ, Rodríguez D et al (2010) Reproducibility of echocardiographic measurements of epicardial fat thickness. Int J Cardiol 141:311–313
11. Bertaso AG, Bertol D, Duncan BB, Foppa M (2013) Epicardial fat: definition, measurements and systematic review of main outcomes. Arq Bras Cardiol 101:e18–e28
12. Gorter PM, van Lindert AS, de Vos AM et al (2008) Quantification of epicardial and peri-coronary fat using cardiac computed tomography; reproducibility and relation with obesity and metabolic syndrome in patients suspected of coronary artery disease. Atherosclerosis 197:896–903
13. Alexopoulos N, McLean DS, Janik M, Arepalli CD, Stillman AE, Raggi P (2010) Epicardial adipose tissue and coronary artery plaque characteristics. Atherosclerosis 210:150–154
14. Wu FZ, Huang YL, Wang YC et al (2013) Impact of location of epicardial adipose tissue, measured by coronary artery calcium-scoring computed tomography on obstructive coronary artery disease. Am J Cardiol 112:943–949
15. Bettencourt N, Toschke AM, Leite D et al (2012) Epicardial adipose tissue is an independent predictor of coronary atherosclerotic burden. Int J Cardiol 158:26–32
16. Hell MM, Ding X, Rubeaux M et al (2016) Epicardial adipose tissue volume but not density is an independent predictor for myocardial ischemia. J Cardiovasc Comput Tomogr 10:141–149
17. Bos D, Leening MJG (2018) Leveraging the coronary calcium scan beyond the coronary calcium score. Eur Radiol 28:3082–3087
18. Brouha SS, Nguyen P, Bettencourt R, Sirlin CB, Loomba R (2018) Increased severity of liver fat content and liver fibrosis in non-alcoholic fatty liver disease correlate with epicardial fat volume in type 2 diabetes: a prospective study. Eur Radiol 28:1345–1355
19. Berrington de González A, Mahesh M, Kim KP et al (2009) Projected cancer risks from computed tomographic scans performed in the United States in 2007. Arch Intern Med 169:2071–2077
20. Xie X, Zhao Y, de Bock GH et al (2013) Validation and prognosis of coronary artery calcium scoring in nontriggered thoracic computed tomography: systematic review and meta-analysis. Circ Cardiovasc Imaging 6:514–521
21. Hecht HS, Cronin P, Blaha MJ et al (2017) 2016 SCCT/STR guidelines for coronary artery calcium scoring of noncontrast noncardiac chest CT scans: a report of the Society of Cardiovascular Computed Tomography and Society of Thoracic Radiology. J Cardiovasc Comput Tomogr 11:74–84
22. van Hamersvelt RW, Willemink MJ, Takx RA et al (2014) Cardiac valve calcifications on low-dose unenhanced ungated chest computed tomography: inter-observer and inter-examination reliability, agreement and variability. Eur Radiol 24:1557–1564
23. Kammerlander AA, Aschauer S, Zotter-Tufaro C et al (2017) Diameter of the pulmonary artery in relation to the ascending aorta: association with cardiovascular outcome. Radiology 284:685–693
24. Wolff L, Bos D, Murad SD et al (2016) Liver fat is related to cardiovascular risk factors and subclinical vascular disease: the Rotterdam study. Eur Heart J Cardiovasc Imaging 17:1361–1367
25. Simon-Yarza I, Viteri-Ramírez G, Saiz-Mendiguren R, Slon-Roblero PJ, Paramo M, Bastarrika G (2012) Feasibility of epicardial adipose tissue quantification in non-ECG-gated low-radiation-dose CT: comparison with prospectively ECG-gated cardiac CT. Acta Radiol 53:536–540
26. Lee KC, Yong HS, Lee J, Kang EY, Na JO (2018) Is the epicardial adipose tissue area on non-ECG gated low-dose chest CT useful for predicting coronary atherosclerosis in an asymptomatic population considered for lung cancer screening? Eur Radiol. https://doi.org/10.1007/s00330-018-5562-4
27. Leipsic J, Abbara S, Achenbach S et al (2014) SCCT guidelines for the interpretation and reporting of coronary CT angiography: a report of the Society of Cardiovascular Computed Tomography Guidelines Committee. J Cardiovasc Comput Tomogr 8:342–358
28. Raff GL, Abidov A, Achenbach S et al (2009) SCCT guidelines for the interpretation and reporting of coronary computed tomographic angiography. J Cardiovasc Comput Tomogr 3:122–136
29. Hulten EA, Carbonaro S, Petrillo SP, Mitchell JD, Villines TC (2011) Prognostic value of cardiac computed tomography angiography: a systematic review and meta-analysis. J Am Coll Cardiol 57:1237–1247
30. Bland JM, Altman DG (1986) Statistical methods for assessing agreement between two methods of clinical measurement. Lancet 1:307–310
31. Bland JM, Altman DG (1999) Measuring agreement in method comparison studies. Stat Methods Med Res 8:135–160
32. Hughes-Austin JM, Dominguez A 3rd, Allison MA et al (2016) Relationship of coronary calcium on standard chest CT scans with mortality. JACC Cardiovasc Imaging 9:152–159
33. DeLong ER, DeLong DM, Clarke-Pearson DL (1988) Comparing the areas under two or more correlated receiver operating characteristic curves: a nonparametric approach. Biometrics 44:837–845
34. La Grutta L, Toia P, Farruggia A et al (2016) Quantification of epicardial adipose tissue in coronary calcium score and CT coronary angiography image data sets: comparison of attenuation values, thickness and volumes. Br J Radiol 89:20150773
35. Bucher AM, Joseph Schoepf U, Krazinski AW et al (2015) Influence of technical parameters on epicardial fat volume quantification at cardiac CT. Eur J Radiol 84:1062–1067
36. Ito T, Suzuki Y, Ehara M et al (2013) Impact of epicardial fat volume on coronary artery disease in symptomatic patients with a zero calcium score. Int J Cardiol 167:2852–2858
37. Tsushima H, Yamamoto H, Kitagawa T et al (2015) Association of epicardial and abdominal visceral adipose tissue with coronary atherosclerosis in patients with a coronary artery calcium score of zero. Circ J 79:1084–1091